JACS JOURNAL OF THE AMERICAN CHEMICAL SOCIETY

pubs.acs.org/JACS Article

Mechanochemistry of Pterodactylane

Matías Horst, Jan Meisner, Jinghui Yang, Tatiana B. Kouznetsova, Stephen L. Craig,* Todd J. Martínez,* and Yan Xia*

Cite This: *J. Am. Chem. Soc.* 2024, 146, 884−891

Read Online

ACCESS | Metrics & More | Article Recommendations | Supporting Information

ABSTRACT: Pterodactylane is a [4]-ladderane with substituents on the central rung. Comparing the mechanochemistry of the [4]-ladderane structure when pulled from the central rung versus the end rung revealed a striking difference in the threshold force of mechanoactivation: the threshold force is dramatically lowered from 1.9 nN when pulled on the end rung to 0.7 nN when pulled on the central rung. We investigated the bicyclic products formed from the mechanochemical activation of pterodactylane experimentally and computationally, which are distinct from the mechanochemical products of ladderanes being activated from the end rung. We compared the products of pterodactylane's mechanochemical and thermal activation to reveal differences and similarities in the mechanochemical and thermal pathways of pterodactylane transformation. Interestingly, we also discovered the presence of elementary steps that are accelerated or suppressed by force within the same mechanochemical reaction of pterodactylane, suggesting rich mechanochemical manifolds of multicyclic structures. We rationalized the greatly enhanced mechanochemical reactivity of the central rung of pterodactylane and discovered force-free ground state bond length to be a good low-cost predictor of the threshold force for cyclobutane-based mechanophores. These findings advance our understanding of mechanochemical reactivities and pathways, and they will guide future designs of mechanophores with low threshold forces to facilitate their applications in force-responsive materials.

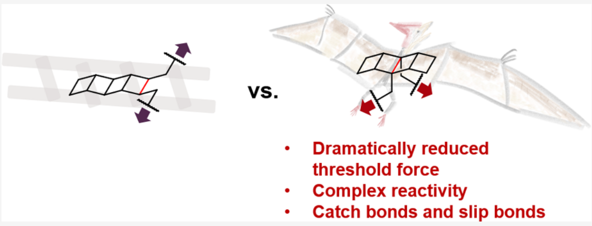

- Dramatically reduced threshold force
- Complex reactivity
- Catch bonds and slip bonds

■ INTRODUCTION

Mechanical work has emerged as a strategy for energy input to activate distinct covalent chemistry. In addition to parameters commonly considered for thermal and photochemical reaction manifolds, such as reaction temperatures and time scales, polymer mechanochemistry encompasses many parameters that are unique to how the force is transduced onto the reactive moieties or mechanophores. A key parameter for polymer mechanochemistry is threshold force, the force at which the rate of mechanophore reaction becomes competitive with the rate of polymer elongation.[1] For a given mechanophore, the threshold force changes as a function of the mechanical context, specifically the loading rate or strain rate that the polymer strand experiences in the environment being considered. High loading rates are found in the sonication of solutions of individual polymers or in ballistic impact events or shock wave loading in bulk materials. In general, these higher loading rates lead to higher threshold forces for a particular mechanophore.[2,3] Lower threshold forces are observed in slower loadings that take more time but that are more typical of the day-to-day environment experienced by many of the materials that we use routinely. The strain rates of approximately 0.1−10 s^{-1} accessed by single molecule force spectroscopy (SMFS) are relevant to many common use applications. SMFS also provides perhaps the most accurate experimental method of quantifying threshold force or force-rate behavior of mechanophores more generally.

Lowering the threshold force is often highly desired as it reflects an enhanced mechanical response. Changes to molecular structures adjacent to or remote from the bonds being activated can alter the reaction manifold, raising or lowering the threshold force and varying the product distribution. For example, the SMFS threshold forces of electrocyclic ring opening of *gem*-dihalocyclopropanes along a polymer main chain have been shown to dramatically decrease with subtle changes in the structure of the chemically inactive substituent adjacent to the mechanophore group. Five-membered cycloalkanes lower the threshold force relative to linear alkenes, and *E*-alkenes lower the threshold force relative to *Z*-alkenes.[4,5] Similar "lever-arm effects" have been invoked in the isomerization of main chain alkenes.[6] Remote electronic effects can also influence the force necessary for reactivity, as was shown for spiropyran,[7] and they can even change the mechanism of reaction itself, as was shown for C−C bond scission between an N-heterocyclic carbene and an aryl ring.[8] Regioisomers that undergo unique reactivity and force sensitivity depending upon the location and direction of the

Received: October 11, 2023
Revised: December 8, 2023
Accepted: December 11, 2023
Published: December 22, 2023

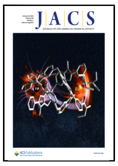

applied force vector, rather than merely its magnitude, are particularly paradigmatic examples in polymer mechanochemistry, and they advance our understanding and control of force-triggered reactivity. Naphthopyran isomers have been reported for which one isomer undergoes mechanochemical reactivity and the other does not.[9] Regioisomers can often undergo mechanochemical reactivity at different forces, as has been reported for spiropyran,[10,11] furan/maleimide adducts,[12] and rubredoxin.[13]

We previously explored the mechanochemistry of [4]-ladderane (Figure 1) with the end rung connected to the polymer main chain.[14,15] Pterodactylane, a [4]-ladderane structure with substituents on the central rung, was first synthesized in 1976 specifically to better understand the kinetics of σ-bond dissociation in fused cyclobutane ring systems.[16] Its structure intrigued us to wonder how pulling the same ladderane structure at different locations affects its mechanochemistry. Upon scission of the first bond in a mechanophore, internal strain must then be redistributed onto adjacent bonds. Breaking the central bond of pterodactylane would introduce four equivalent, formally symmetric C−C σ-bonds into the polymer main chain. In addition to comparing the threshold force required for mechanoactivation of the central versus end rung, we were curious about whether additional reactivity would be possible and what products might result from subsequent reactions after the first bond breaks. Herein, we report the distinct mechanochemical reactivities of [4]-ladderane when the force is applied to the central rung vs the end rung, revealed by single molecule force spectroscopy (SMFS), sonication experiments, and force-modified potential energy surface[17] (FMPES) calculations.

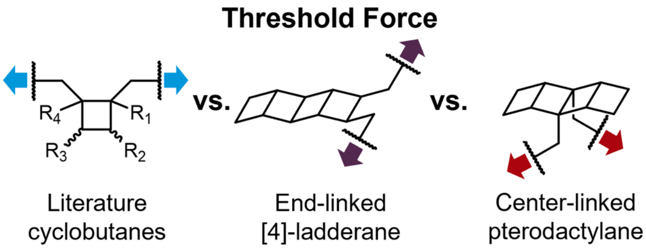

Figure 1. Comparison of the structures of [4]-ladderane, linked to the polymer chain by the end rung, and pterodactylane, linked to the polymer chain by the central rung.

■ RESULTS AND DISCUSSION

We sought to compare the threshold forces for activation when pulling [4]-ladderane at the middle vs end rung using SMFS. We first synthesized pterodactylenediol **1** by reacting 2.5 equiv of (cyclobutadiene)iron tricarbonyl[18] with dimethylacetylene dicarboxylate following a previously reported procedure.[19] To ease the analysis of mechanochemical products that are expected to contain alkenes and for a better comparison with our previously characterized [4]-ladderane, we decided to hydrogenate the cyclobutenes in **1** (Scheme 1). An initial attempt at hydrogenation of **1** using Pd/C for 4 h gave a low yield of the desired compound and a large amount of ring-opened side products. By limiting the reaction time to about 1 h, we were able to achieve complete hydrogenation without noticeable ring opening to give saturated pterodactylanediol **2** in 93% yield. Next, we used esterification of **2** with 4-pentenoic anhydride to generate diene **3**, which was subsequently cyclized via ring-closing metathesis (RCM) to give macrocyclic alkene **4**. Finally, entropy-driven ring-opening metathesis copolymerization (ED-ROMP) of **4** with epoxy-cyclooctene gave polymer **P1**, which is well suited for SMFS measurement.[20,21]

Scheme 1. Synthesis of Pterodactylane-Containing Polymers P1, P3, and P4 and Structure of the Reported [4]-Ladderane Polymer P2[15]

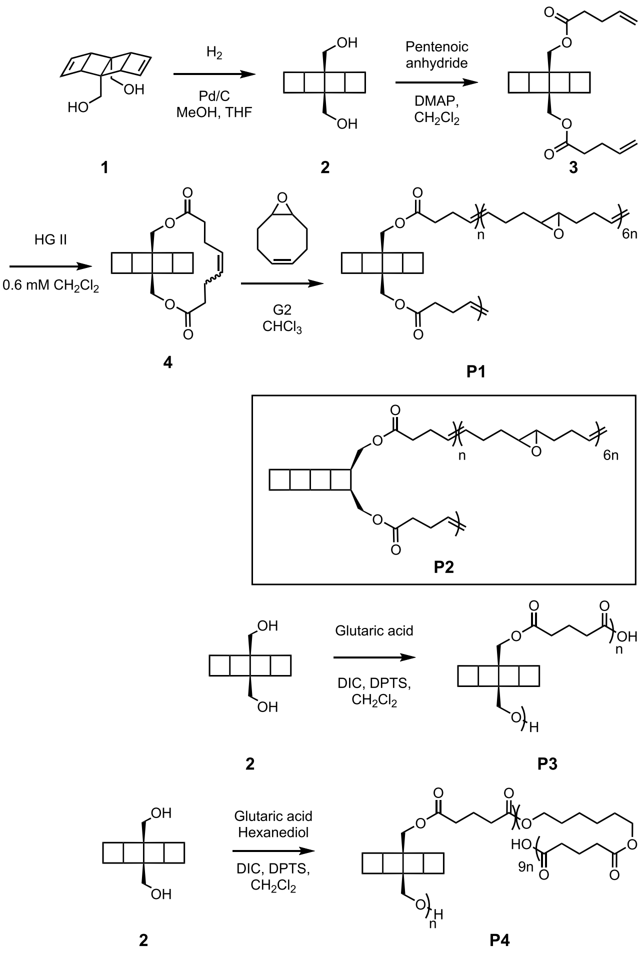

An isomeric polymer **P2** was previously synthesized using the same procedure.[15] **P1** and **P2** have the same polymer main chain structures, the same substituents on the [4]-ladderane structure, similar MWs, and similar ladderane fractions (13 and 14 mol %, respectively); these polymers differ only in the connectivity by which the [4]-ladderane motif is attached to the polymer main chain. Individual strands of each polymer were extended via SMFS in toluene at room temperature using a constant retraction rate of 300 nm/s (Figure 2).[22] Upon application of force, a change in contour length was observed, corresponding to a force-triggered reaction. The threshold forces were obtained by averaging many retraction curves, and changes in contour length were determined by fitting the pre- and post-transition regions of the force curves to extended freely jointed chain models.[23,24] When force is applied at the end rung of [4]-ladderane, a threshold force for activation of 1910 ± 14 pN was observed[15]; in contrast, when force is applied at the middle rung, a plateau was observed at a strikingly low force of 709 ± 40 pN, associated with a contour length change of 2.4 ± 0.5%. Moving the location of force applied from the end to the middle of [4]-ladderane

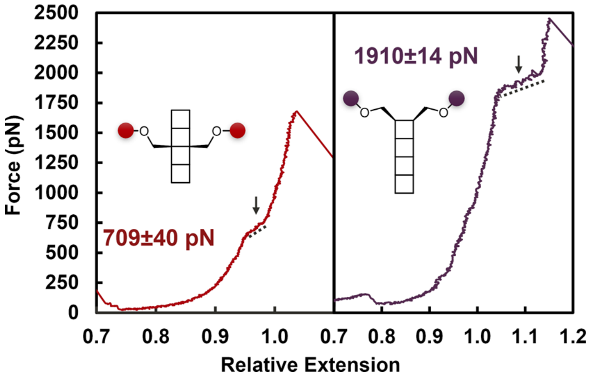

Figure 2. Representative single molecule force−extension curves of **P1** (red) and a previously reported ladderane polymer[15] **P2** (purple) normalized to extension at 1 nN. A dashed line is included as a visual aid to highlight the plateau corresponding to mechanophore activation.

dramatically lowered the threshold force for mechanoactivation by 1.2 nN, and the force is lower than that for any reported isolated or fused cyclobutane ring with similar substituents at which the force is applied.[25]

Mechanophores with low activation threshold forces are highly desired for the development of materials with a greater force response.[26] To rationalize the low force required for the reactivity of pterodactylane within concepts of the physical organic canon, we turned to the recently proposed tension model of bond activation (TMBA).[27] This model deploys two key parameters that together are highly predictive of threshold force: the Hookean spring constant of the first broken bond and the potential energy difference between the reactant and the diradical intermediate. We calculated the spring constant of the central rung of pterodactylane to be 11.0 nN/Å (Figure S25) and found it to be among the lowest for cyclobutane-based mechanophores studied in developing the TMBA model, which ranges from 7.0 to 44.3 nN/Å. Only a cyclobutane with flanking phenyl groups has a lower value of 7.0 nN/ Å.[1,27] We also calculated the change in force-free potential energy upon conversion of **5** to **6** to be 26.1 kcal/mol. This was also among the lowest for homolytic C−C bond scission events evaluated by the TMBA model, which ranged from 17.2 to 67.8 kcal/mol. The small Δ*E* of pterodactylane can be understood as resulting from destabilization of the middle rung of pterodactylane by high ring strain and the vicinal quaternary centers and stabilization of the bond-cleaved diradical intermediate **6** by tertiary substitution at the radical carbons.

An intriguing comparison is between ladderane being pulled at the central or end rung and another strained compound with multiple fused cyclobutanes, cubane. The end rung of [4]-ladderane has a calculated potential energy of 55.3 kcal/mol for bond cleavage and a spring constant of 20.9 nN/ Å,[27] both of which are significantly greater than those for the central rung, reflecting the diminished steric crowding around the end rung and decreased radical stability upon its cleavage. The threshold force for mechanoactivation of 1,2-cubane was recently reported to be 1.55 nN under the same SMFS conditions, still significantly higher than that for pterodactylane.[25] While cubane has a similar calculated potential energy difference to pterodactylane for breaking the first bond, it shows a significantly greater spring constant.[28] The rigid cubic structure of cubane acts as a brace, which may explain its higher spring constant than pterodactylane.

We were further motivated to study whether simple structural elements could be empirical predictors of threshold forces of mechanoactivation for cyclobutane-based mechanophores. Including the pterodactylane disclosed herein, seven cyclobutane mechanophores have been quantitatively studied by SMFS at room temperature and 300 nm/second elongation rates in the literature.[1,15,25] We calculated optimized geometries for model analogues of these seven mechanophores at applied forces of 0.0, 0.5, 1.0, and 2.0 nN[17] and then explored the correlations between threshold force and different structural parameters of these molecules, such as the length of the scissile bond and strain localization (Figure 3 and Figures S19−S24). X-ray crystallography of [4]-ladderane diol showed the central bond of the molecular ladder to be slightly longer than the rest of the rungs,[15] and this result is consistent with the relative bond lengths in pterodactylane diol **2** by *ab initio* calculations. Bond length has been speculated to influence the ring-opening forces of cyclobutanes,[29] and we indeed found a strong inverse correlation between the computed length of the scissile bond at 0.0 nN or 2.0 nN and experimentally measured threshold force. Force-free ground state bond length appears to be a good low-cost predictor of the threshold force of the closely structurally related cyclobutane mechanophores that have been measured by SMFS.

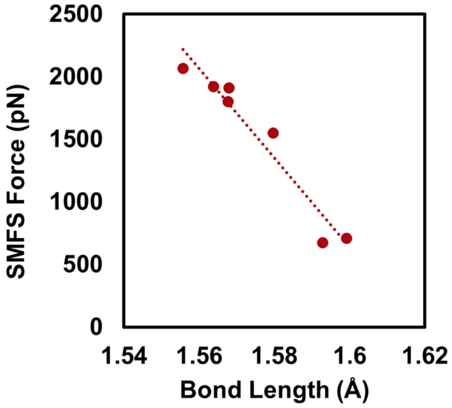

Figure 3. Computed force-free bond length compared with the threshold force measured using SMFS for cyclobutane-based mechanophores. The dashed line shows a linear fit of the data.

We next turned to study the mechanochemistry of pterodactylane using ultrasonication, which is a widely used technique to apply high forces to polymers dissolved in solution. Given the range of alkenes that may conceivably be produced upon the mechanoactivation of pterodactylane, we sought to prepare polymers with a saturated main chain structure to simplify the characterization of the reaction products. Hydrogenation of **P1** to saturate the main chain alkenes is not feasible because pterodactylene degrades during Pd/C hydrogenation at a time scale faster than the hydrogenation of polymer main chain alkenes. Consequently, we used polycondensation to construct multimechanophore polymer **P3** with a saturated polyester main chain for the sonochemical study.

Polymer **P3** was sonicated in THF at 3−5 °C, and samples were removed at 60 and 120 min and then precipitated for GPC and ^{1}H NMR analysis. Upon sonication, we observed the growth of broad signals in the alkenyl region of the ^{1}H NMR spectrum (Figure 4a). Distinctively, a peak at 5.78 ppm

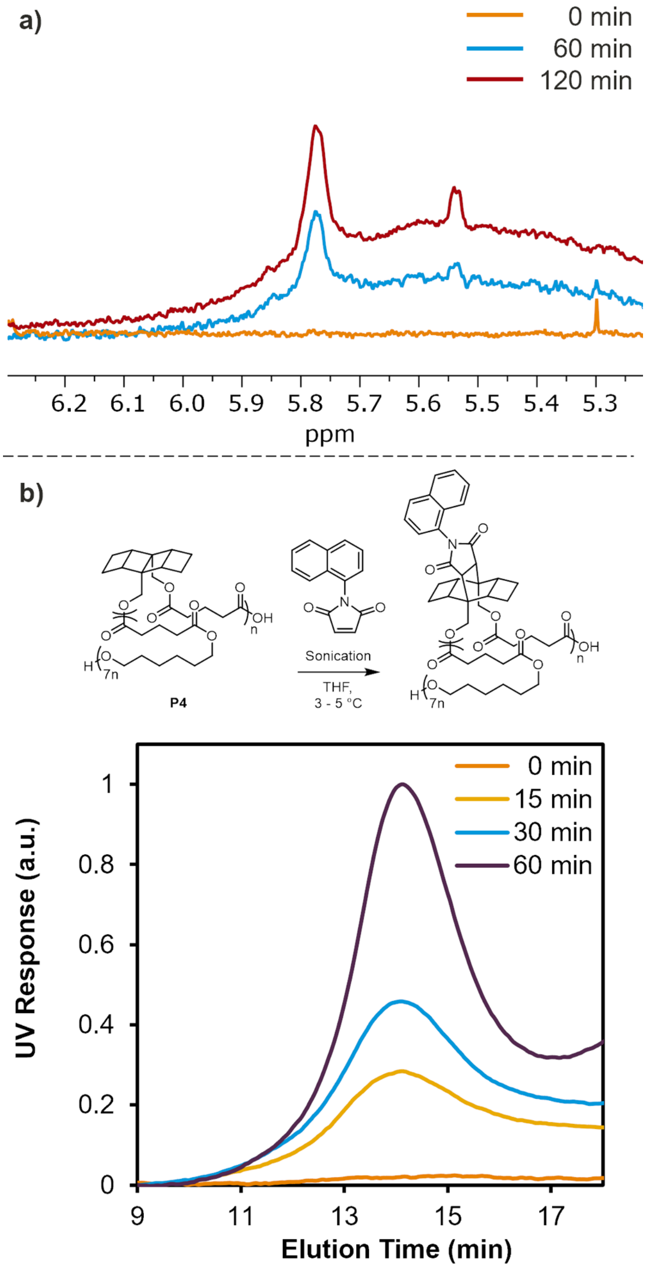

Figure 4. (a) Overlaid alkenyl region of ^{1}H NMR spectra of **P3** following 0, 60, or 120 min of sonication in THF. (b) Increasing absorption intensity at 355 nm in the GPC peak of **P4** after being sonicated in the presence of 100 equiv of naphthyl maleimide and then thrice precipitated.

appeared after 60 min of sonication. After 120 min of sonication, another peak at 5.55 ppm also emerged along with increased intensity of the peak at 5.78 ppm and the broad signals in the alkenyl region. Over the course of sonication, we did not observe signals corresponding to terminal alkenes, which would be above 6 ppm, suggesting that the complete unzipping of pterodactylane into a tetraene species (Figure S17) is unlikely. This absence is also consistent with the length change of polymers measured in SMFS, given the computed contour lengths of potential repeat unit structures (Table S4).

Scheme 2. Computation-Assisted Understanding of Mechanochemical Reaction of Pterodactylane, Showing Transformation of 5 to Diradical 6 and then Bicyclic Diene 7[a]

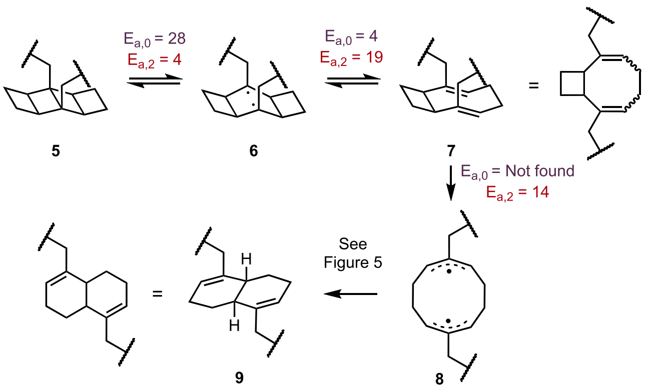

[a] Breaking of an additional bond forms allylic diradical **8**, which then undergoes rapid reaction to form [4.4.0]-bicyclodecadiene **9.** Included are the computed free energies of activation for the forward reaction of each elementary transformation at 0.0 or 2.0 nN in kcal/mol.

The first bond cleavage of the central rung in pterodactylane **5** would generate diradical intermediate **6** (Scheme 2). In our previous study, the diradical generated by unzipping [4]-ladderane from the end rung is very short-lived, as suggested by calculation, and it was not able to be experimentally trapped.[14] We were curious about the stability and reactivity of the initial diradical **6** formed in pterdactylane mechanoactivation. Inspired by previous work to trap mechanochemically generated *ortho*-quinodimethides by maleimides,[30,31] we sonicated **P4** in the presence of 100 equiv of naphthyl maleimide. Samples were intermittently removed, precipitated from methanol, and characterized by GPC/UV−vis spectroscopy (Figure 4b) and NMR spectroscopy. An absorption peak at 355 nm, which corresponds to the absorption of naphthyl maleimide, grew as sonication time increased. Based on UV−vis detection, this peak coeluted with the polymer peak revealed by the RI detector, suggesting trapping of the diradical by naphthyl maleimide. Under the same experimental conditions, no such labeling was observed during the sonication of a polyester control sample that does not contain pterodactylane (Figure S6). Computational investigation of the addition of naphthyl maleimide to pterodactylane diradical **6** further suggests that the reaction has a minimal barrier (Figure S9). After a first C−C bond is formed, a second, barrierless C−C bond formation can occur, leading to a bicyclic product. These computational results are consistent with the experimental observation of diradical trapping by naphthyl maleimide during the sonication of **P4**.

To further identify the possible mechanochemical products of pterodactylane, we sought to investigate the thermal product of pterodactylanediol **2**. Thermolysis of **2** at 80 °C in deuterated methanol resulted in one major distinct alkene ^{1}H NMR peak at 5.78 ppm, and the thermal product formation followed first-order kinetics with a rate constant of 0.061 h^{-1}. Two alkenyl signals were observed in the ^{13}C NMR spectrum of the thermal product. We identified the product structure to be [2.6.0]-bicyclodecadienediol, the dihydroxy analogue of **7** with a *Z* configuration based on ^{1}H−^{13}C HSQC and 2D NOESY analyses (Figures S40−S43). Pterodactylane, either as a small molecule or incorporated into a polymer, gave the same observed alkenyl proton peak upon thermolysis (Figures S44 and S45). Based on the same chemical shift and peak shape, we

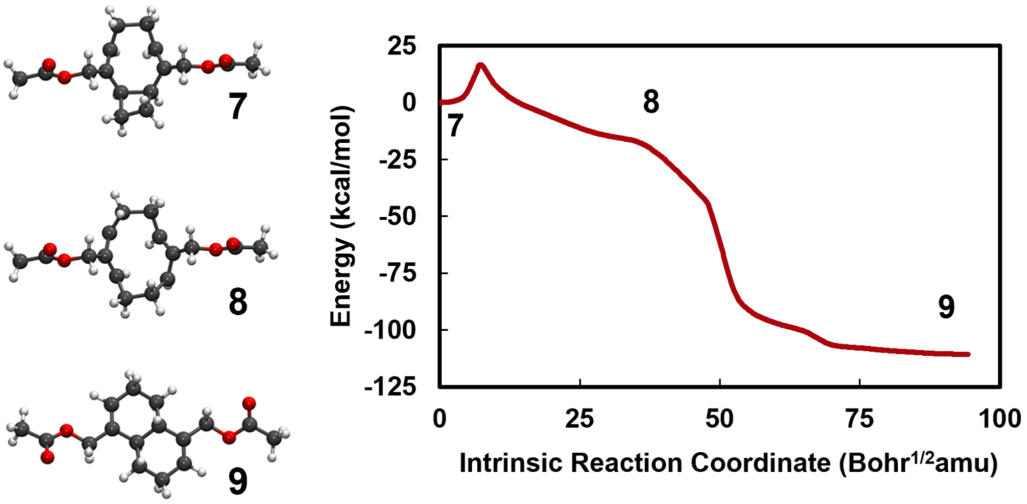

Figure 5. Intrinsic reaction coordinate for the transformation of **7** to **9** via the diradical structure **8** at a pulling force of 2.0 nN.

attributed the major signal at 5.78 ppm observed in the sonication of pterodactylane to the bicyclodecadiene structure **7**.

We calculated the force-modified potential energy surface (FM-PES) to develop a better understanding of other plausible reaction products. Within the FM-PES model, the potential energy landscape is distorted by an external force. This allows force-dependent reaction barriers to be calculated without requiring artificial division into purely thermal and purely mechanical reactions. We optimized stationary point structures using B3LYP-D3/6-31G(d) and calculated energies of activation over a range of forces (SI Section 4.2). Upon formation of an initial diene **7**, additional reactions were computationally found to be thermally accessible under 2.0 nN force: diene **7** can undergo a third bond scission to form allylic diradical **8**, which can then recombine to give **9**, a bicyclic [4.4.0]decadiene with *anti* bridgehead hydrogens (Figure 5). This requires substantial conformational distortion of diradical **8** (Scheme S1). While for the direct bond scission, transition state structures were only found for forces of 1.5 nN and above, other pathways for the formation of **9** involving stereochemical isomerization of diene **7** were also found. Further details about these reaction steps can be found in Scheme S2 and Table S1. Based on the low energy barrier computed under force for the conversion from **7** to **9** and the chemical shift of a similar reported bicyclic alkene[32] (Scheme S4), we propose **9** to be the most parsimonious structure corresponding to the signals at 5.55 ppm.

We then delved into the FM-PES of the mechanochemical activation of pterodactylane to better understand the energetics, kinetics, and force sensitivity of the involved elementary steps. First, we considered the breaking of the central rung in pterodactylane (Scheme 2). A monotonic decrease in the activation energy with increasing force was observed for this first bond-breaking event that generated diradical **6**, supporting the mechanochemical nature of the reaction (Figure 6, green trace). Using the experimentally observed threshold force of 0.71 nN, a free activation energy of 18.7 kcal/mol was obtained by computation for the conversion of **5** to **6**. We were surprised to observe a contrasting trend in the breaking of a second, adjacent rung following formation of the first diradical: increasing forces led to increased activation energies (Figure 6, blue trace). Interactions for which bond scission is suppressed rather than accelerated by applied force are known as catch bonds and have been widely observed in biophysics.[33] Catch bonds have been observed in DNA binding,[34] adjacent strands in a β-barrel,[35] adhesin−saccharide interactions,[36] and cytoskeletal protein interactions.[37] Boulatov and co-workers reported a synthetic system with a catch bond character: increasing force from 0.0 to 0.2 nN decelerated the hydrolysis of a siloxane macrocycle.[38] The lack of reactivity in the cycloreversion of an anthracene maleimide Diels−Alder adduct and the retro-[2 + 2] cycloaddition of ketene dimer rings have been explained using catch bond-like reactivity.[39,40]

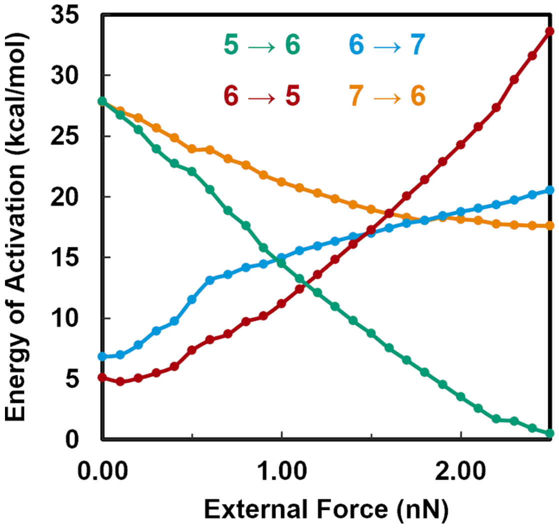

Figure 6. Force-modified free energy barriers of selected pterodactylane reactions, calculated at the B3LYP-D3/6-31(d) level, for the forward reaction of **5** to **6** (green), the reverse reaction of **6** to **5** (red), the forward reaction of **6** to **7** (blue), and the reverse reaction of **7** to **6** (orange). Lines only serve to guide the eye.

To understand this catch bond behavior, we further analyzed the optimized structures of **5**, **6**, and **7** (Figure 7a and Figure S26). As the central rung is broken, the bond length increases (Figure 7b). Conversion of the diradical to the diene results in a further increase in the distance between the carbons of the scissile central rung. However, during this transition from **6** to **7**, the distance between the methylene units alpha to the central rung undergoes contraction. This contraction, as large

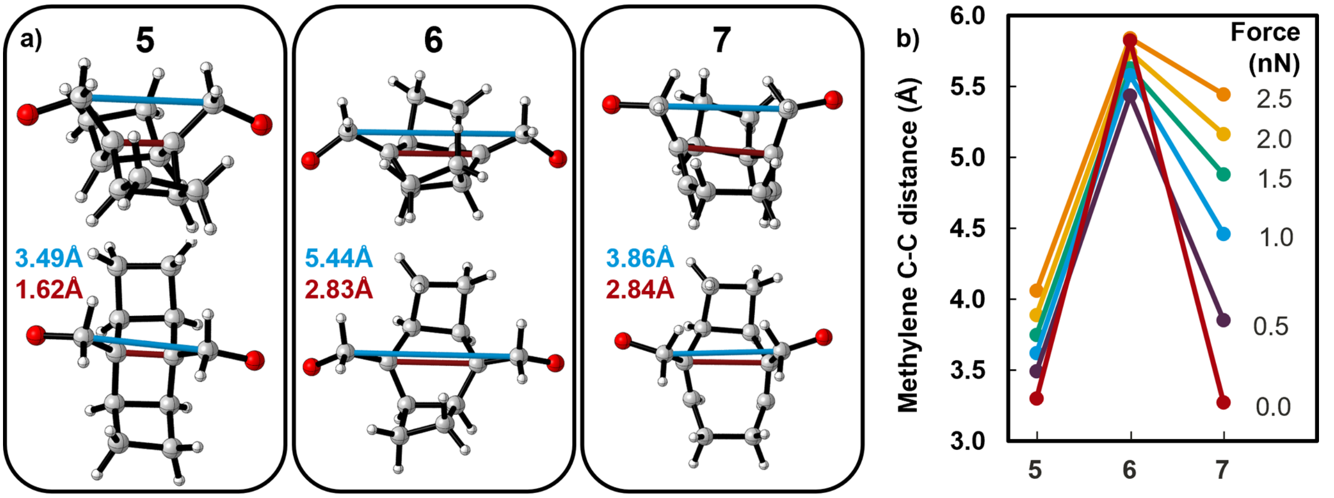

Figure 7. Computationally investigated reactions of pterodactylane showing the initial bond breaking and second bond breaking. Shown at the left are the B3LYP-D3/6-31G(d)-predicted geometries of **5**, **6**, and **7** at 500 pN of applied force (acetyl groups were hidden for clarity). The interatomic distances are shown for carbons of the scissile central rung (red) and the attached methylene carbons (blue). At the right, the computed interatomic distances for these methylene carbons are shown for **5**, **6**, and **7** at 0.0, 0.5, 1.0, 1.5, 2.0, and 2.5 nN of applied force (lines are added only to guide the eye).

as 1.6 Å at 0.5 nN, requires work to be done against the applied pulling force, and consequently, increased forces suppress the conversion of **6** to **7**. Since both the forward reaction of **6** to **7** and the reverse reaction of **6** to **5** are decelerated by force, we might expect that force increases the radical lifetime of **6**. The presence of elementary steps that are accelerated or suppressed by force within the mechanochemical reaction of pterodactylane suggests the rich mechanochemical manifolds of multicyclic structures.

■ CONCLUSIONS

Mechanochemical C−C bond scission in pterodactylane occurs at a force dramatically lower than that in its structural isomer, [4]-ladderane. After the first central bond cleavage on pterodactylane, multiple reactions with a broad range of force sensitivities proceed to several bicyclic dienes. Among these reactions, some are found to be force-accelerated, while some are force-decelerated. The low threshold force for the mechanoactivation of pterodactylane is attributed to both the high mechanical sensitivity and low potential energy barrier for cleaving the central rung. These findings from the study of the mechanochemistry of pterodactylane suggest the engaging complexity of multicyclic mechanophores and may inspire designs of new mechanophores that undergo mechanoactivation at low forces. The computational study also suggests that consideration of the full topographical complexity of potential energy surfaces under the distortions of force is necessary to understand the landscape of mechanochemistry.

■ ASSOCIATED CONTENT

Supporting Information

The Supporting Information is available free of charge at https://pubs.acs.org/doi/10.1021/jacs.3c11293.

> Detailed descriptions of synthetic procedures, experimental methods, ^{1}H and ^{13}C NMR spectra of new compounds and polymers, GPC analysis, SMFS results, and computational details (PDF)

■ AUTHOR INFORMATION

Corresponding Authors

Stephen L. Craig − *Department of Chemistry, Duke University, Durham, North Carolina 27708, United States;* orcid.org/0000-0002-8810-0369; Email: stephen.craig@duke.edu

Todd J. Martínez − *Department of Chemistry, Stanford University, Stanford, California 94305, United States; SLAC National Accelerator Laboratory, Menlo Park, California 94025, United States;* orcid.org/0000-0002-4798-8947; Email: toddmtz@stanford.edu

Yan Xia − *Department of Chemistry, Stanford University, Stanford, California 94305, United States;* orcid.org/0000-0002-5298-748X; Email: yanx@stanford.edu

Authors

Matías Horst − *Department of Chemistry, Stanford University, Stanford, California 94305, United States;* orcid.org/0000-0002-9794-5355

Jan Meisner − *Department of Chemistry, Stanford University, Stanford, California 94305, United States; Institute for Physical Chemistry, Department of Chemistry, Heinrich-Heine-Universität Düsseldorf, Düsseldorf D-40225, Germany;* orcid.org/0000-0002-1301-2612

Jinghui Yang − *Department of Chemistry, Stanford University, Stanford, California 94305, United States;* orcid.org/0000-0002-6957-6265

Tatiana B. Kouznetsova − *Department of Chemistry, Duke University, Durham, North Carolina 27708, United States*

Complete contact information is available at: https://pubs.acs.org/10.1021/jacs.3c11293

Notes

The authors declare no competing financial interest.

■ ACKNOWLEDGMENTS

This work was supported by U.S. Army Research Office under grant numbers W911NF-15-1-0525 (Y.X. and T.J.M.) and CHE-1808518 (S.L.C.). M.H. was supported by a Center for

Molecular Analysis and Design grant and a National Defense Science and Engineering Graduate Fellowship. J.M. thanks Deutsche Forschungsgemeinschaft (project number 419817859) for financial support. J.Y. was supported by a Stanford Graduate Fellowship. The ALS is supported by the Director, Office of Science, Office of Basic Energy Science, of the U.S. Department of Energy under contract no. DE-AC02-05CH11231. This work used the XStream computational resource, supported by the National Science Foundation Major Research Instrumentation program (ACI-1429830). Some of the computing for this project was performed on the Sherlock cluster. We would like to thank Stanford University and Stanford Research Computing Center for providing computational resources and support that contributed to these research results. This work was supported by the Vincent Coates Foundation Mass Spectrometry Laboratory, Stanford University Mass Spectrometry (RRID:SCR_017801) utilizing the Waters SQD2 LC/MS system (RRID:SCR_022217).

■ REFERENCES

(1) Bowser, B. H.; Wang, S.; Kouznetsova, T. B.; Beech, H. K.; Olsen, B. D.; Rubinstein, M.; Craig, S. L. Single-Event Spectroscopy and Unravelling Kinetics of Covalent Domains Based on Cyclobutane Mechanophores. *J. Am. Chem. Soc.* **2021**, *143* (13), 5269−5276.

(2) Bell, G. Models for the Specific Adhesion of Cells to Cells. *Science* **1978**, *200* (4342), 618−627.

(3) Merkel, R.; Nassoy, P.; Leung, A.; Ritchie, K.; Evans, E. Energy Landscapes of Receptor−Ligand Bonds Explored with Dynamic Force Spectroscopy. *Nature* **1999**, *397* (6714), 50−53.

(4) Klukovich, H. M.; Kouznetsova, T. B.; Kean, Z. S.; Lenhardt, J. M.; Craig, S. L. A Backbone Lever-Arm Effect Enhances Polymer Mechanochemistry. *Nat. Chem.* **2013**, *5* (2), 110−114.

(5) Wang, J.; Kouznetsova, T. B.; Kean, Z. S.; Fan, L.; Mar, B. D.; Martínez, T. J.; Craig, S. L. A Remote Stereochemical Lever Arm Effect in Polymer Mechanochemistry. *J. Am. Chem. Soc.* **2014**, *136* (43), 15162−15165.

(6) Huang, W.; Zhu, Z.; Wen, J.; Wang, X.; Qin, M.; Cao, Y.; Ma, H.; Wang, W. Single Molecule Study of Force-Induced Rotation of Carbon−Carbon Double Bonds in Polymers. *ACS Nano* **2017**, *11* (1), 194−203.

(7) Barbee, M. H.; Kouznetsova, T.; Barrett, S. L.; Gossweiler, G. R.; Lin, Y.; Rastogi, S. K.; Brittain, W. J.; Craig, S. L. Substituent Effects and Mechanism in a Mechanochemical Reaction. *J. Am. Chem. Soc.* **2018**, *140* (40), 12746−12750.

(8) Nixon, R.; De Bo, G. Three Concomitant C−C Dissociation Pathways during the Mechanical Activation of an N-Heterocyclic Carbene Precursor. *Nat. Chem.* **2020**, *12* (9), 826−831.

(9) Robb, M. J.; Kim, T. A.; Halmes, A. J.; White, S. R.; Sottos, N. R.; Moore, J. S. Regioisomer-Specific Mechanochromism of Naphthopyran in Polymeric Materials. *J. Am. Chem. Soc.* **2016**, *138* (38), 12328−12331.

(10) Gossweiler, G. R.; Kouznetsova, T. B.; Craig, S. L. Force-Rate Characterization of Two Spiropyran-Based Molecular Force Probes. *J. Am. Chem. Soc.* **2015**, *137* (19), 6148−6151.

(11) Kim, T. A.; Robb, M. J.; Moore, J. S.; White, S. R.; Sottos, N. R. Mechanical Reactivity of Two Different Spiropyran Mechanophores in Polydimethylsiloxane. *Macromolecules* **2018**, *51* (22), 9177−9183.

(12) Stevenson, R.; De Bo, G. Controlling Reactivity by Geometry in Retro-Diels−Alder Reactions under Tension. *J. Am. Chem. Soc.* **2017**, *139* (46), 16768−16771.

(13) Zheng, P.; Chou, C.-C.; Guo, Y.; Wang, Y.; Li, H. Single Molecule Force Spectroscopy Reveals the Molecular Mechanical Anisotropy of the FeS_4 Metal Center in Rubredoxin. *J. Am. Chem. Soc.* **2013**, *135* (47), 17783−17792.

(14) Chen, Z.; Zhu, X.; Yang, J.; Mercer, J. A. M.; Burns, N. Z.; Martinez, T. J.; Xia, Y. The Cascade Unzipping of Ladderane Reveals Dynamic Effects in Mechanochemistry. *Nat. Chem.* **2020**, *12* (3), 302−309.

(15) Horst, M.; Yang, J.; Meisner, J.; Kouznetsova, T. B.; Martínez, T. J.; Craig, S. L.; Xia, Y. Understanding the Mechanochemistry of Ladder-Type Cyclobutane Mechanophores by Single Molecule Force Spectroscopy. *J. Am. Chem. Soc.* **2021**, *143* (31), 12328−12334.

(16) Martin, H.-D.; Hekman, M. Four Linearly Annelated Cyclobutane Rings: The Tetracyclo[4.4.0.02,5.07,10]Decane System. *Angew. Chem., Int. Ed. Engl.* **1976**, *15* (7), 431−432.

(17) Ong, M. T.; Leiding, J.; Tao, H.; Virshup, A. M.; Martínez, T. J. First Principles Dynamics and Minimum Energy Pathways for Mechanochemical Ring Opening of Cyclobutene. *J. Am. Chem. Soc.* **2009**, *131* (18), 6377−6379.

(18) Pettit, R.; Henergy, J. Cyclobutadieneiron Tricarbonyl. *Org. Synth.* **1970**, *50*, 21.

(19) Meinwald, J.; Mioduski, J. Tetracyclo[4.4.0.0.2,507,10]-Decanes: Direct Synthesis from Cyclobutadieneiron Tricarbonyl and Dienophilic Acetylenes. *Tetrahedron Lett.* **1974**, *15* (44), 3839−3842.

(20) Lee, B.; Niu, Z.; Wang, J.; Slebodnick, C.; Craig, S. L. Relative Mechanical Strengths of Weak Bonds in Sonochemical Polymer Mechanochemistry. *J. Am. Chem. Soc.* **2015**, *137* (33), 10826−10832.

(21) Bowser, B. H.; Craig, S. L. Empowering Mechanochemistry with Multi-Mechanophore Polymer Architectures. *Polym. Chem.* **2018**, *9* (26), 3583−3593.

(22) Kouznetsova, T. B.; Wang, J.; Craig, S. L. Combined Constant-Force and Constant-Velocity Single-Molecule Force Spectroscopy of the Conrotatory Ring Opening Reaction of Benzocyclobutene. *ChemPhysChem* **2017**, *18* (11), 1486−1489.

(23) Smith, S. B.; Cui, Y.; Bustamante, C. Overstretching B-DNA: The Elastic Response of Individual Double-Stranded and Single-Stranded DNA Molecules. *Science* **1996**, *271* (5250), 795−799.

(24) Oesterhelt, F.; Rief, M.; Gaub, H. E. Single Molecule Force Spectroscopy by AFM Indicates Helical Structure of Poly(Ethylene-Glycol) in Water. *New J. Phys.* **1999**, *1*, 6−6.

(25) Wang, L.; Zheng, X.; Kouznetsova, T. B.; Yen, T.; Ouchi, T.; Brown, C. L.; Craig, S. L. Mechanochemistry of Cubane. *J. Am. Chem. Soc.* **2022**, *144* (50), 22865−22869.

(26) Lloyd, E. M.; Vakil, J. R.; Yao, Y.; Sottos, N. R.; Craig, S. L. Covalent Mechanochemistry and Contemporary Polymer Network Chemistry: A Marriage in the Making. *J. Am. Chem. Soc.* **2023**, *145*, 751.

(27) Sun, Y.; Kevlishvili, I.; Kouznetsova, T.; Burke, Z.; Craig, S.; Kulik, H.; Moore, J. The Tension Activated Carbon−Carbon Bond. *ChemRxiv*. **2023**. DOI: 10.26434/chemrxiv-2023-rzwhn.

(28) The calculated cubane in ref 27 has dicarboxylate substituents, while the ladderane and pterodactylane structures calculated here have alkyl substituents. The different substituents may exert minor influences on the free energy and spring constants, but the qualitative trend is expected to remain constant. See compounds **15** and **19** of ref 27.

(29) Kryger, M. J.; Munaretto, A. M.; Moore, J. S. Structure−Mechanochemical Activity Relationships for Cyclobutane Mechanophores. *J. Am. Chem. Soc.* **2011**, *133* (46), 18992−18998.

(30) Potisek, S. L.; Davis, D. A.; Sottos, N. R.; White, S. R.; Moore, J. S. Mechanophore-Linked Addition Polymers. *J. Am. Chem. Soc.* **2007**, *129* (45), 13808−13809.

(31) Hickenboth, C. R.; Moore, J. S.; White, S. R.; Sottos, N. R.; Baudry, J.; Wilson, S. R. Biasing Reaction Pathways with Mechanical Force. *Nature* **2007**, *446* (7134), 423−427.

(32) Tori, M.; Sono, M.; Nishigaki, Y.; Nakashima, K.; Asakawa, Y. Studies on the Liverwort Sesquiterpene Alcohol Tamariscol. Synthesis and Absolute Configuration. *J. Chem. Soc. Perkin 1* **1991**, *2*, 435.

(33) Thomas, W. E.; Vogel, V.; Sokurenko, E. Biophysics of Catch Bonds. *Annu. Rev. Biophys.* **2008**, *37* (1), 399−416.

(34) Albrecht, C.; Blank, K.; Lalic-Mülthaler, M.; Hirler, S.; Mai, T.; Gilbert, I.; Schiffmann, S.; Bayer, T.; Clausen-Schaumann, H.; Gaub, H. E. DNA: A Programmable Force Sensor. *Science* **2003**, *301* (5631), 367−370.

(35) Brockwell, D. J.; Paci, E.; Zinober, R. C.; Beddard, G. S.; Olmsted, P. D.; Smith, D. A.; Perham, R. N.; Radford, S. E. Pulling Geometry Defines the Mechanical Resistance of a β-Sheet Protein. *Nat. Struct. Mol. Biol.* **2003**, *10* (9), 731−737.

(36) Thomas, W.; Forero, M.; Yakovenko, O.; Nilsson, L.; Vicini, P.; Sokurenko, E.; Vogel, V. Catch-Bond Model Derived from Allostery Explains Force-Activated Bacterial Adhesion. *Biophys. J.* **2006**, *90* (3), 753−764.

(37) Huang, D. L.; Bax, N. A.; Buckley, C. D.; Weis, W. I.; Dunn, A. R. Vinculin Forms a Directionally Asymmetric Catch Bond with F-Actin. *Science* **2017**, *357* (6352), 703−706.

(38) Akbulatov, S.; Tian, Y.; Huang, Z.; Kucharski, T. J.; Yang, Q.-Z.; Boulatov, R. Experimentally Realized Mechanochemistry Distinct from Force-Accelerated Scission of Loaded Bonds. *Science* **2017**, *357* (6348), 299−303.

(39) Konda, S. S. M.; Brantley, J. N.; Varghese, B. T.; Wiggins, K. M.; Bielawski, C. W.; Makarov, D. E. Molecular Catch Bonds and the Anti-Hammond Effect in Polymer Mechanochemistry. *J. Am. Chem. Soc.* **2013**, *135* (34), 12722−12729.

(40) Groote, R.; Szyja, B. M.; Leibfarth, F. A.; Hawker, C. J.; Doltsinis, N. L.; Sijbesma, R. P. Strain-Induced Strengthening of the Weakest Link: The Importance of Intermediate Geometry for the Outcome of Mechanochemical Reactions. *Macromolecules* **2014**, *47* (3), 1187−1192.

https://doi.org/10.1021/jacs.3c11293